Electron-wall interactions and their consequences on transport

Igor D. Kaganovich

Princeton Plasma Physics Laboratory
Princeton, NJ 08543

Outline

Part 1
- Non-Maxwellian EVDF
- Effects of emission on sheath
- Sheath Instability
- Near Wall Conductivity
- Emission from complex surfaces
- Revisiting Pierce Instability

Outline

Part 2

- Validating PIC codes
- 2-3D PPPL-modified LSP
- Anomalous Conductivity
- Spoke

Electron emission from the wall can increase the plasma heat flux to the wall many times

• Without SEE, sheath of space charge near the wall reflects most electrons back to the plasma, thus effectively insulating wall from the plasma (Left Figure)

• SEE reduces the wall potential and allows large electron flux to the wall (Right Figure)
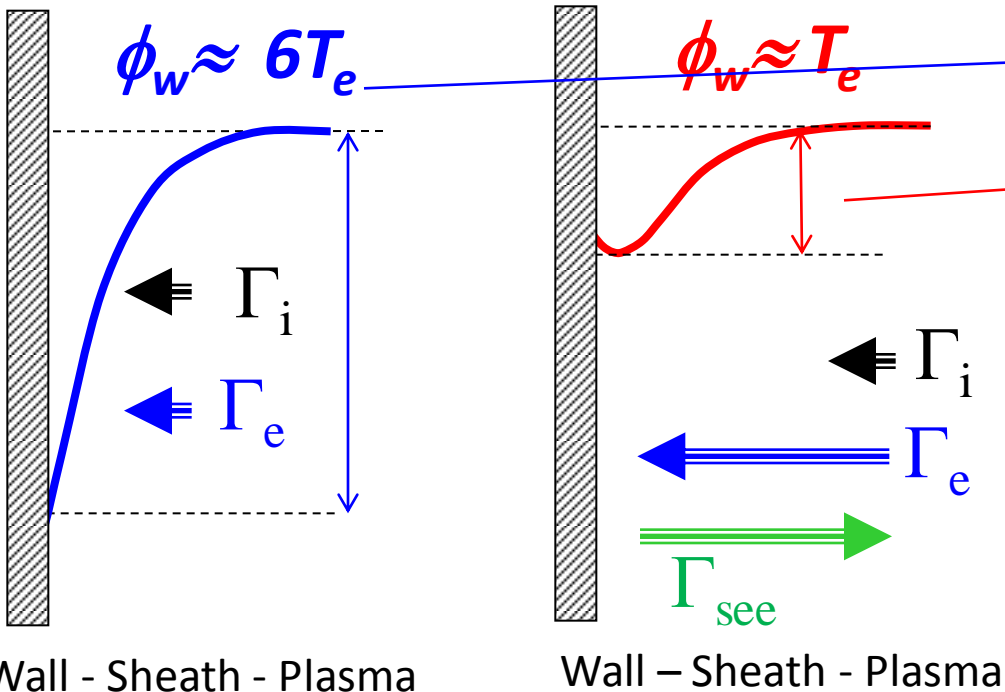
Hall thruster experiments show very different maximum electron temperatures with high and low SEE channel wall materials

$\phi_w \approx 6T_e$

$\phi_w \approx T_e$

Γ_i

Γ_e

Γ_i

Γ_e

Γ_{see}

Wall - Sheath - Plasma

Wall – Sheath - Plasma

Y. Raitses et al., Phys. Plasmas 2005
Y. Raitses et al., IEEE TPS 2011 4
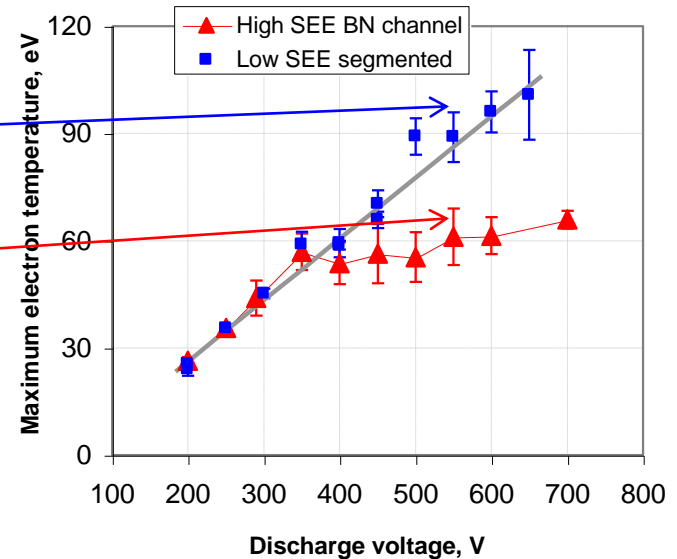
Depletion of fast electrons due to wall losses in a Hall thruster channel

E_z=200 V/cm, B_x=100G

T_{ex}=12eV, Φ_w =19.4eV **!** **Not 5T_e**

Bulk electrons with SEE
Bulk electrons with no SEE
Maxwellian EVDF, **T_{ex}=12eV** *T_z = 36.7 eV*

$\lambda_{ec} \gg H, \Rightarrow$
EVDF is depleted in the B- field direction, $w_x > e\Phi_w$!

EVDF is not depleted in the E-   field direction, $w > e\Phi_w$!
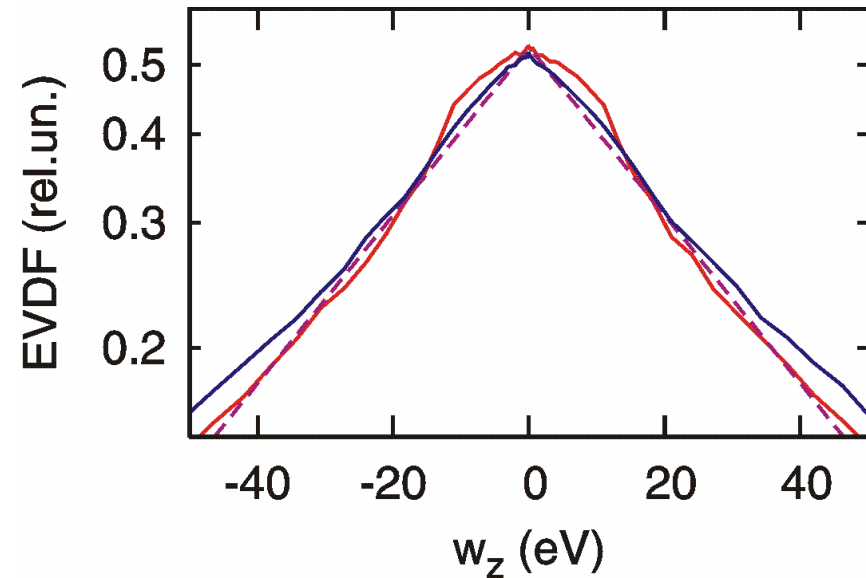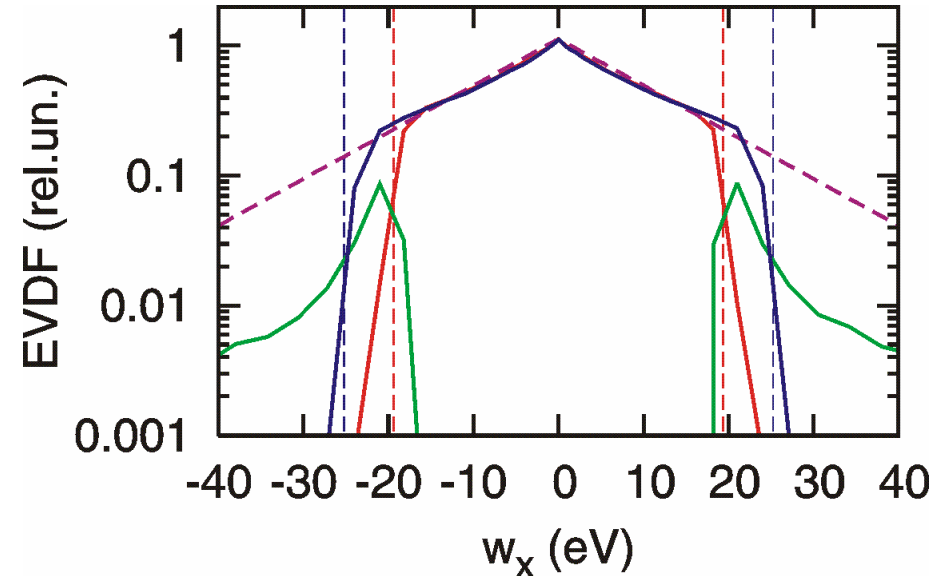
3D view of the EVDF
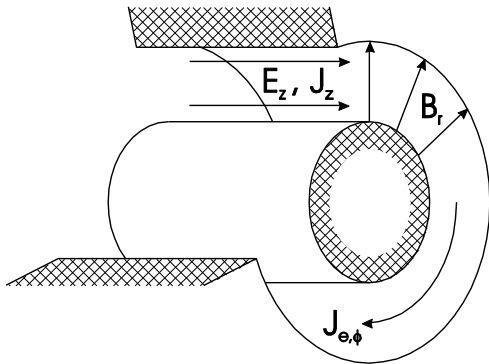
E_z=200 V/cm
B_x=100G

T_x = 12.1 eV

T_z = 36.7 eV

EVDF (rel.un.)

w_x (eV)

w_z (eV)
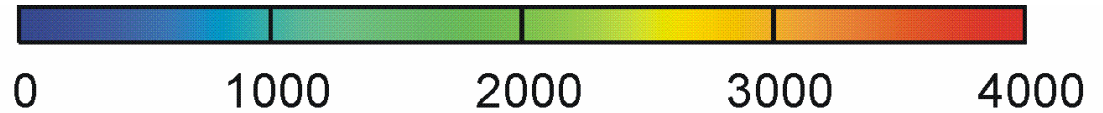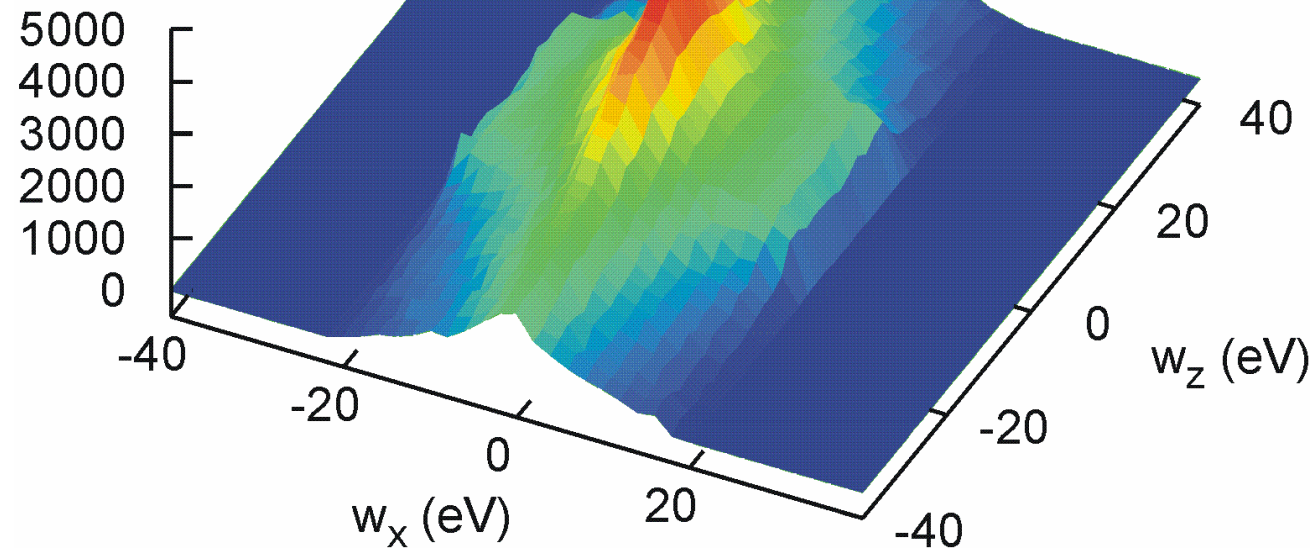
The loss cone concept

- The green circle : particles with energy $w > e\Phi_w$ in the two-dimensional velocity space (v_x, v_z).
- The red section of the circle is the loss cone.
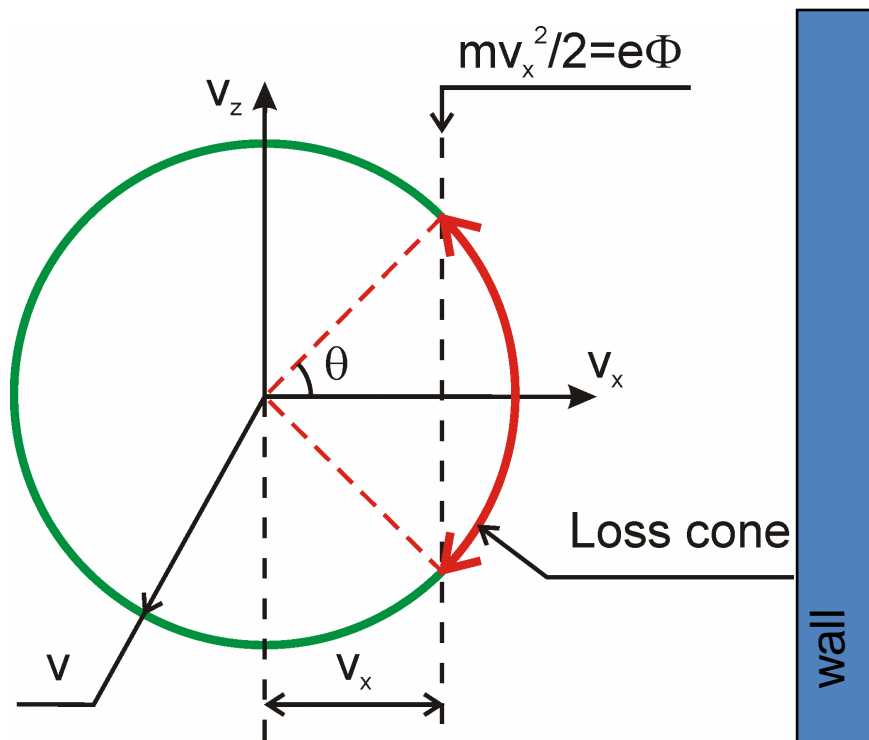
The EVDF in the loss cone is:

- replenished due to the elastic scattering (from outside of the loss cone),
- emptied by the free flight to the walls with the rate determined by the transit time $(\sim H/v_x)$.

Due to the low electron flux to the wall, the wall potential is small.
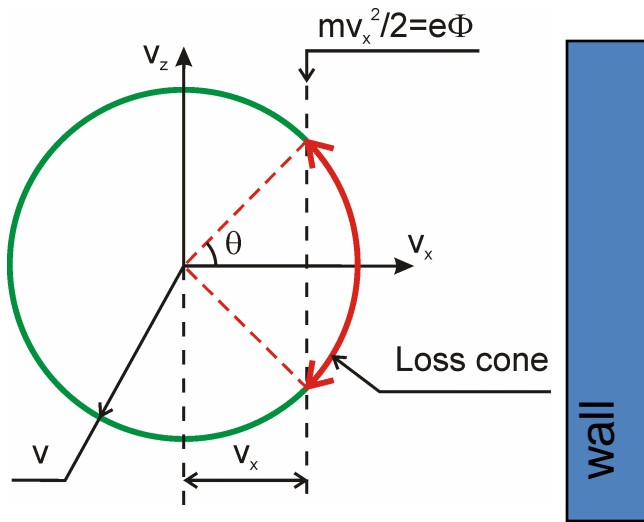
$$\Gamma_e = \left(\frac{H}{8\lambda_c}\right) n_e \sqrt{\frac{8T_{ez}}{\pi m}} \exp\left(-\frac{\Phi}{T_{ez}}\right)$$

Huge reduction due to EVDF depletion

$$\Gamma_{ion} = n\sqrt{\frac{T_e}{M}} \longrightarrow \boxed{\Phi = \frac{T_{ez}}{e} \ln\left(\frac{H}{\lambda_c}\sqrt{\frac{T_{ez}}{T_{ex}}}\sqrt{\frac{M}{2\pi m}}\right) \approx \frac{T_{ez}}{e}}$$

Since $H/\lambda_c \sim 10^{-2}$, the wall potential decreases from $5T_e$ to $1T_e$

From: I.D. Kaganovich, et al., Phys. Plasmas **14**, 057104 (2007).

Secondary electron emission yield from dielectric materials
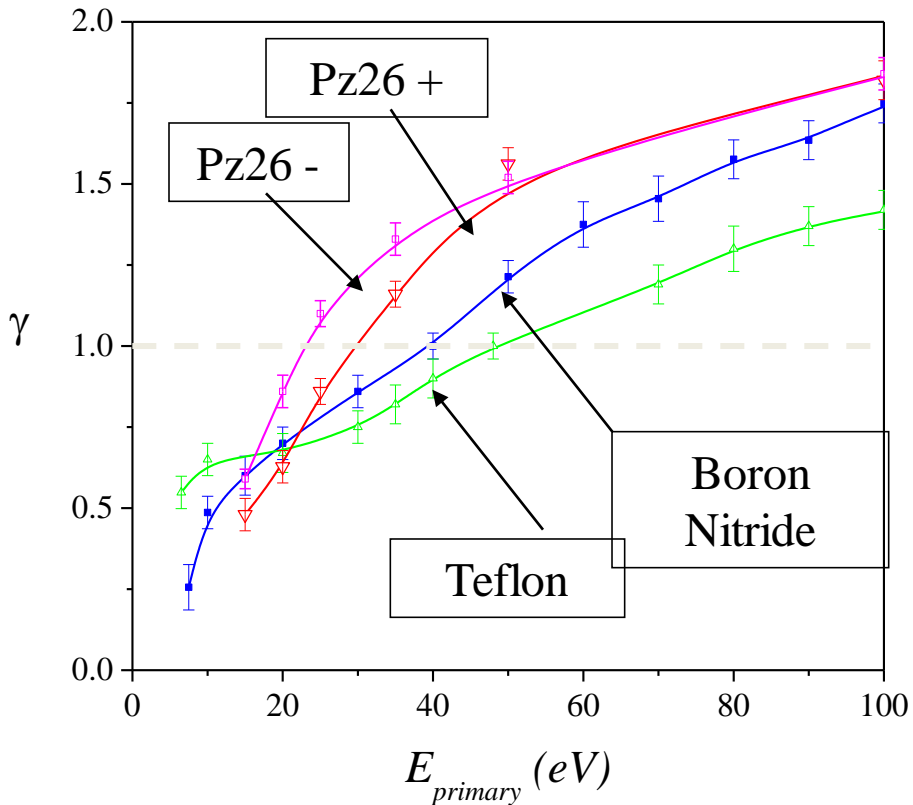
Note:
for Boron Nitride ceramic, if plasma (primary) electrons have Maxwellian electron energy distribution function (EEDF):

$$\gamma(T_e) = 1 \text{ at } T_e = 18.3 \text{ eV}$$

Dunaevsky et al., Phys. Plasmas, 2003

For many plasma applications, electron heat flux to the wall needs to be calculated kinetically
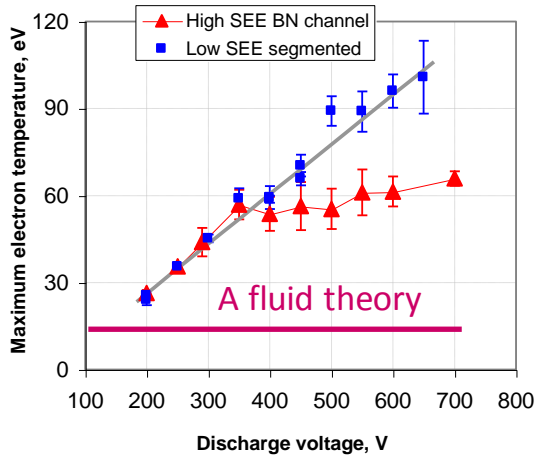
Large quantitative disagreement between experiments and fluid theories for predictions of the electron temperature in Hall thrusters

Y. Raitses et al., Phys. Plasmas 2006
I. Kaganovich et al., Phys. Plasmas 2007
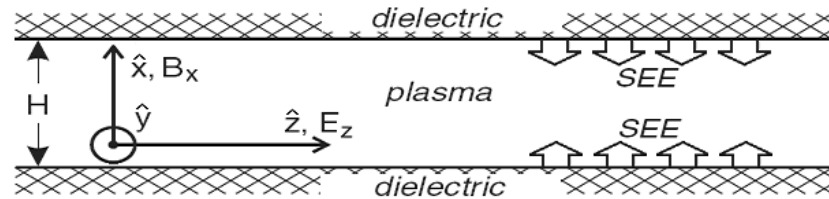
Hall thruster plasma, 2D-EVDF

Isotropic Maxwellian plasma, 2D-EVDF
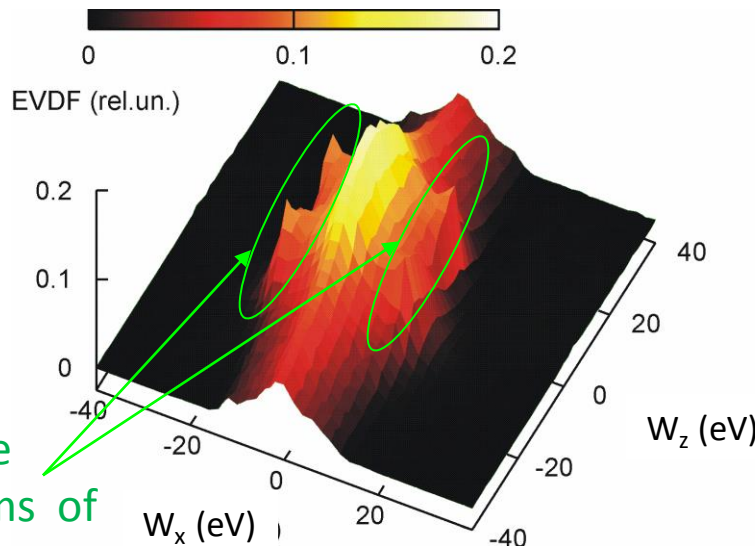
Loss cone and beams of SEE electrons
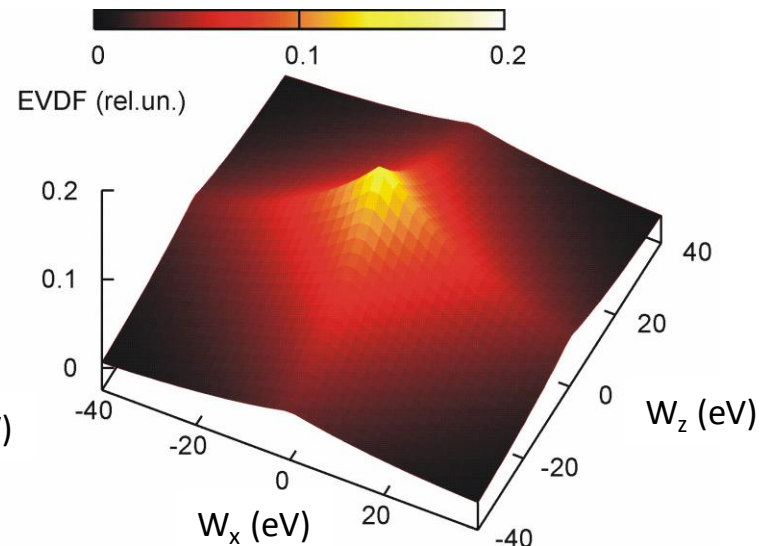
Electron fluxes have several components, including plasma bulk electrons, and counter-streaming beams of SEE electrons from walls

$\varphi(x)$

Γ_{ions}

Γ_{plasma}

Γ_{beam}

Γ_{SEE}

Γ_{ions}

Γ_{plasma}

Γ_{SEE}

Γ_{beam}
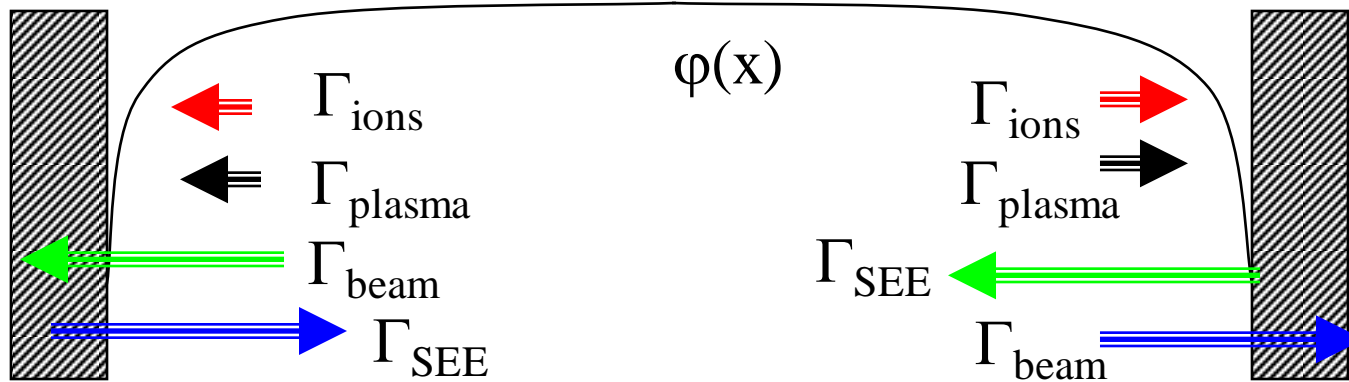
Net secondary electron emission γ_{net} accounts for kinetic effects by separating SEE yield of plasma ($\gamma_{\mathbf{p}}$) and beam electrons ($\gamma_{\mathbf{b}}$)

Total emission coefficient:

$$\gamma_{net} \approx \frac{\gamma_p}{1 + (\gamma_p - \gamma_b)}$$

Note: $\gamma_{\mathbf{net}} > 1$ if $\gamma_{\mathbf{b}} > 1$

SEE Yield as function of incident electron energy

γ 1

Energy of incident electron, eV

11
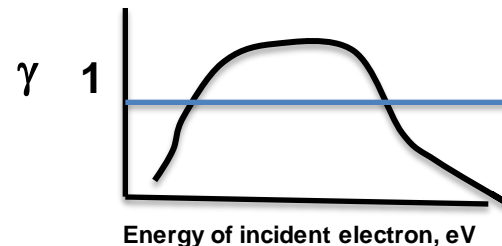
Particle-in-cell (PIC) simulations of plasma in Hall thrusters

12 cm diameter
2 kW Hall thruster
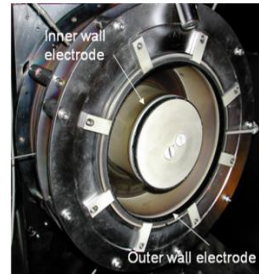
Sheath oscillations occur due to coupling of the sheath potential and non-Maxwellian electron energy distribution function with intense electron beams emitted from the walls.

Left wall **Right wall**

Γ_{ion}

E

E

$\Gamma_{plasma\ e-}$

$\Gamma_{SEE(beam)}$

Γ_{beam}
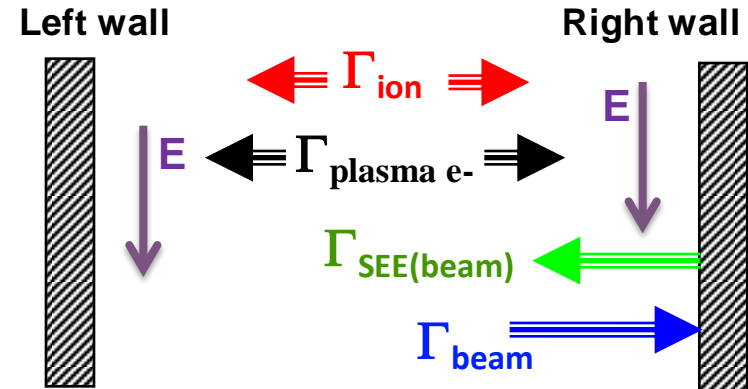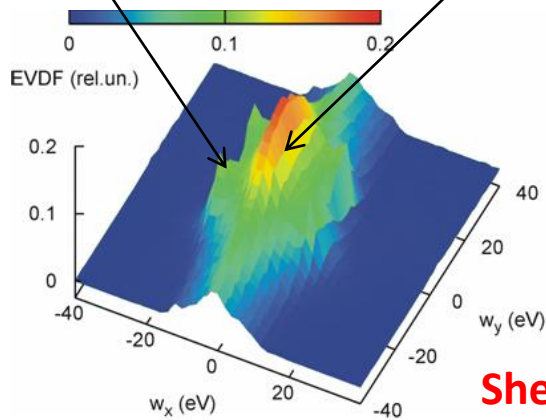
Plasma potential as a function of time

Φ (V)

t (10^{-6} s)
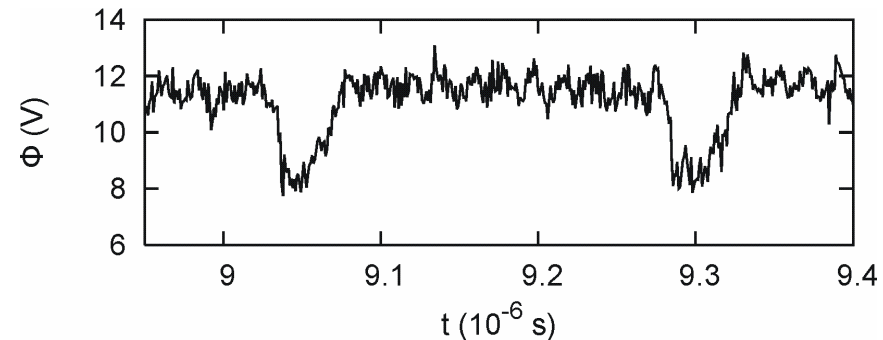
Sheath instability causing fluctuations of plasma potential may enhance electron cross field transport, which leads to reduction of the electric field in plasma channel and accelerated ion energy.

*D. Sydorenko et al, Phys Rev Lett. **103**, 145004 (2009)*

The beams of secondary electrons contribute to the electron cross-field current.

The large flux in the z direction created by the secondary electrons results in additional conductivity in the Hall thruster channel.

The displacement $\rho_c = v_\perp / \omega_c$, $v_\perp = u_d = \dfrac{E_z}{B_x}$ during the flight time H/u$_{bx}$

gives average velocity $\langle u_z \rangle \sim u_d u_{bx} / H\omega_c$ and current $J_{bz} \approx \dfrac{m}{H} \dfrac{\gamma_p}{1-\gamma_b} n_e \sqrt{\dfrac{T_{ex}}{M}} \dfrac{E_z}{B_x^2}$.
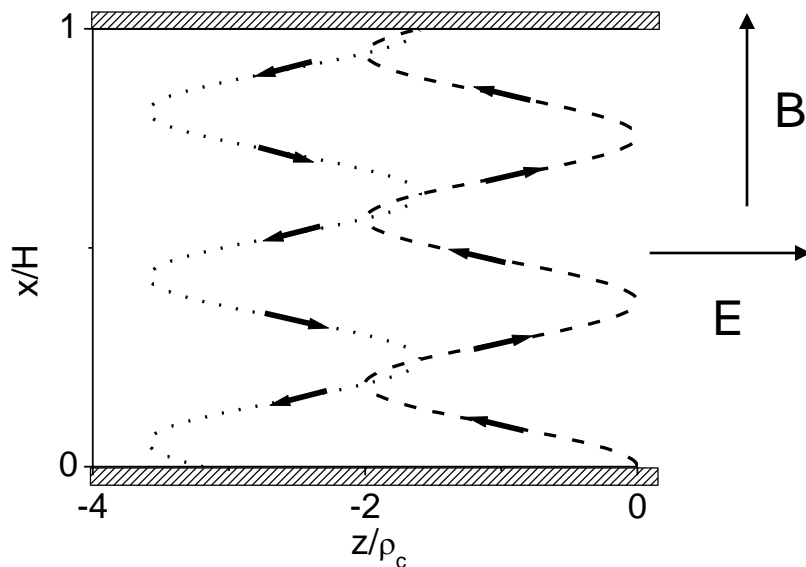
The SEE beam electrons contribute to the reduction of the electric field in the channel.

$$J_{bz} \approx \frac{m}{H} \frac{\gamma_p}{1-\gamma_b} n_e \sqrt{\frac{T_{ex}}{M}} \frac{E_z}{B_x^2}$$

An additional current due to SEE electrons results in lower electric field and, hence, lower electron temperature.

E_Z [V/cm]	52	200
$J_{Z,\text{SEE BEAM}}$ [A/m^2], PIC	2.3	58.4
$J_{Z,\text{SEE BEAM}}$ [A/m^2], estimated	3.2	68.1
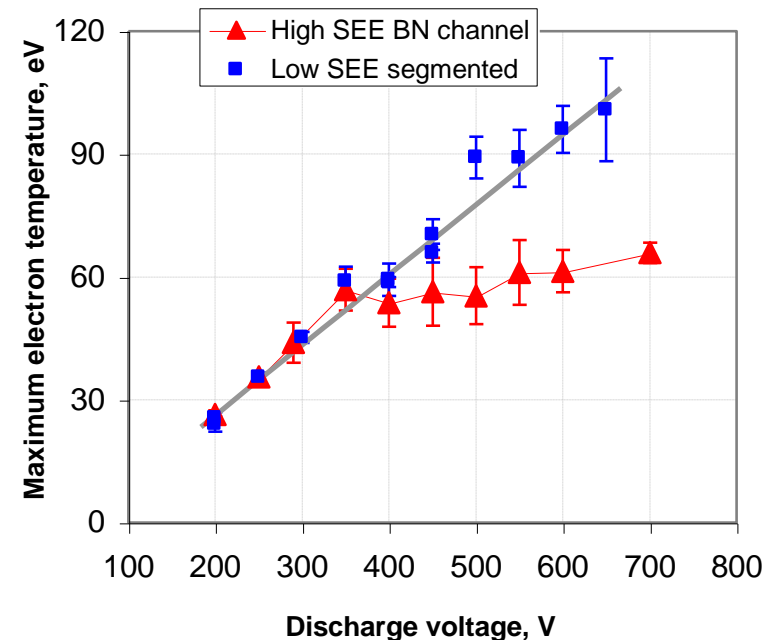
Potential Asymmetry and Electron Motion
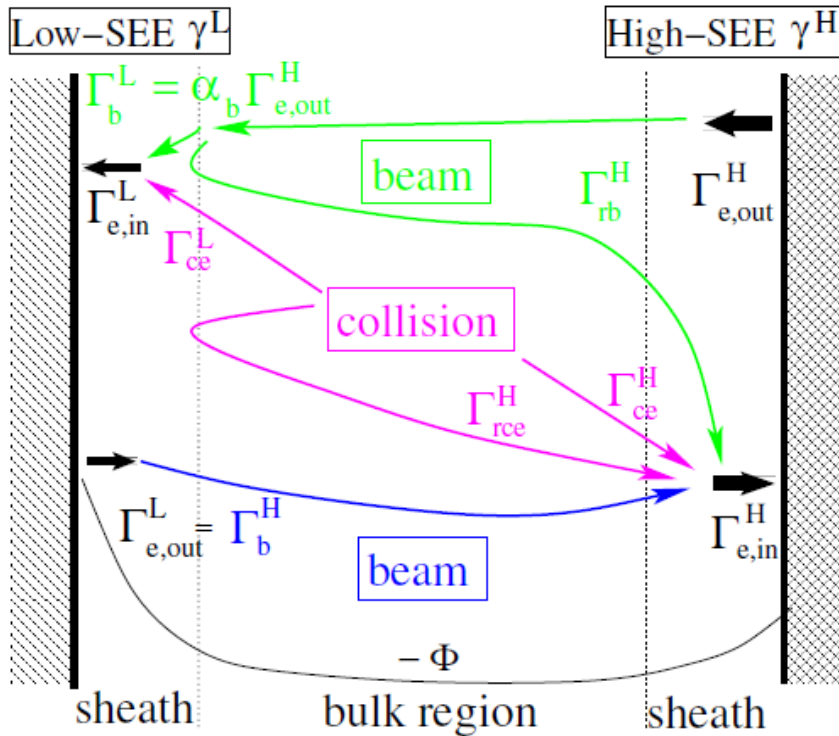
Left SEE yield decreases

More negative charge is accumulated on the left surface

Left wall potential drops

Beam and bulk electrons are reflected by the left sheath

■ The electron flux hitting the wall includes 4 components:

- ❑ Γ_{ce} - Collision-ejected (CE) bulk electrons
- ❑ Γ_{b} - Secondary electrons from the opposite wall
- ❑ Γ_{rce} - CE electrons reflected by the left sheath
- ❑ Γ_{rb} - Secondary electrons reflected by the left sheath

In the asymmetric case we found 2 important new components!

Criterion for onset of sheath oscillations in the presence of strong SEE

Obtained analytical criterion for sheath instability, $dJ/d\varphi > 0 \implies \gamma_{w=\varphi} > 1$.

If sheath potential decreases due to positive charge fluctuations on the wall ($\delta\varphi$), the incident electron flux increases. If secondary electron emission coefficient of additionally released electrons $\gamma_{w=\varphi} > 1$, the emitted electron fluxes increases more than incident flux and wall charges more positively instead of restoring to the original wall charge.

Schematic of instability

Γ_{pe}

SEE

sheath

φ

+

Perturbed surface charge

$\Gamma_{pe} + \delta\Gamma_{pe}$

SEE

$\varphi + \delta\varphi$

−

+

+

Increased perturbation of the surface charge
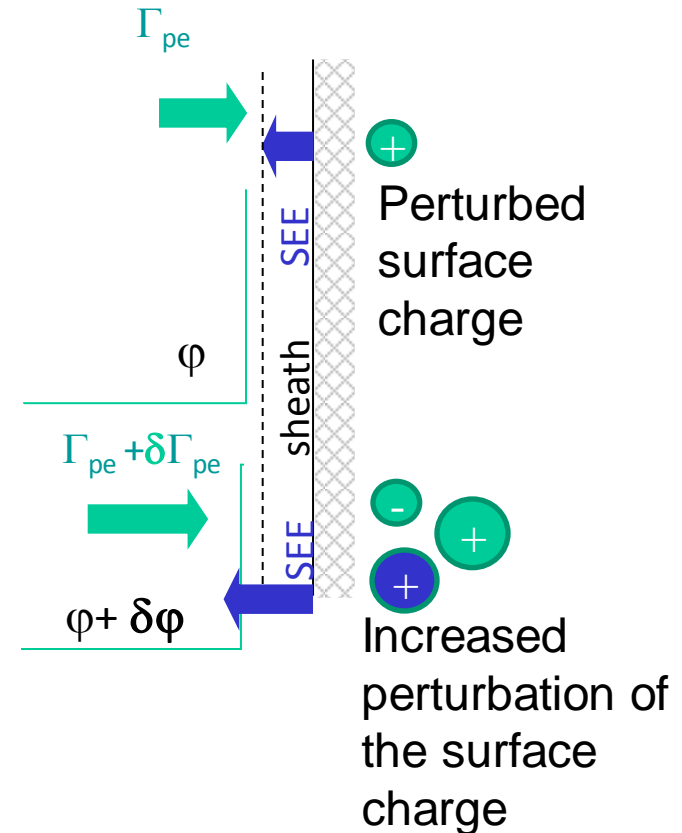
New regime of plasma-wall interaction with a very strong SEE, $\gamma > 1$

The main result - Disappearance of sheaths due to SEE
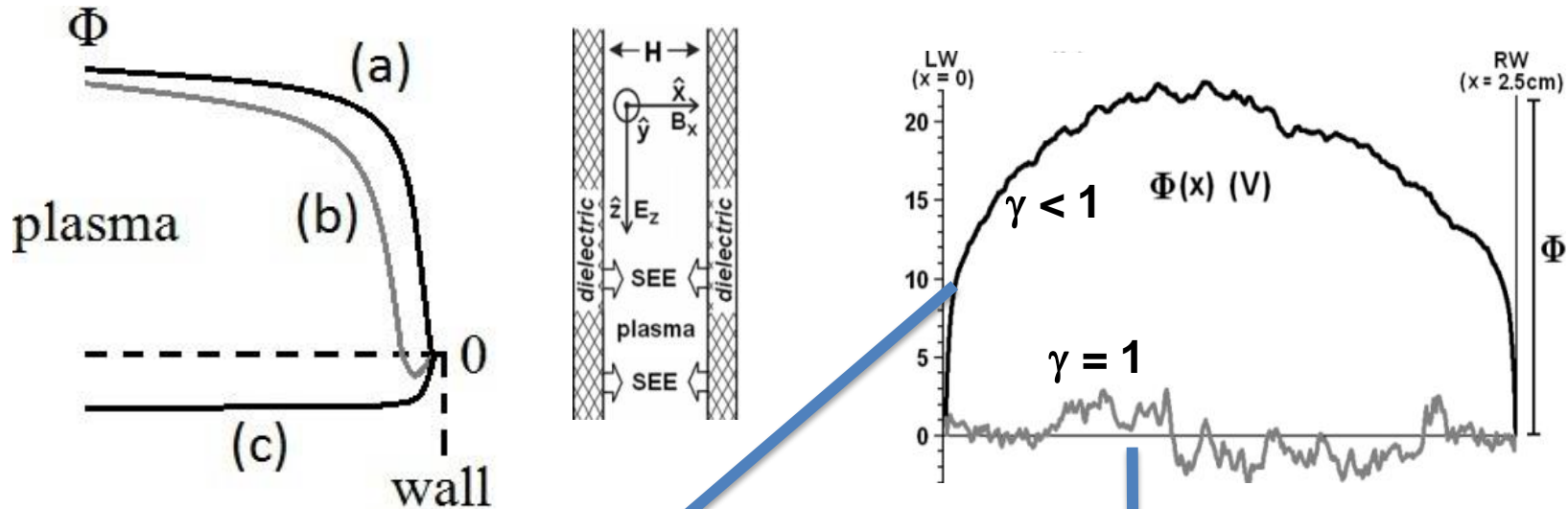
~4 MHz
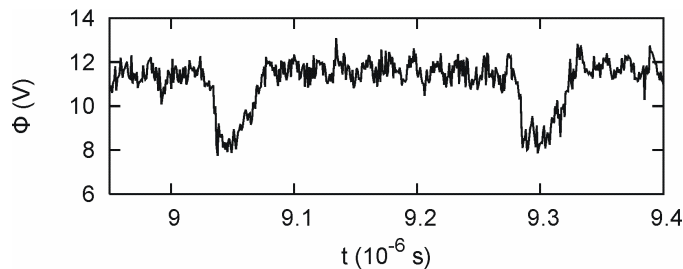
- SEE electrons acquire enough energy from the electric field parallel to the wall causing $\gamma = 1$

- Sheath collapse leads to extreme wall heating by plasma and plasma losses

*M. Campanell et al., Phys. Rev. Lett. **108**, 255001 (2012)*

Plasma potential near emitting surface in complex plasmas

JP Sheehan of UWM conducted experiments at Sandia.

First validation of theoretical predictions that the sheath potential drop near strongly emitting surface vanishes as plasma temperature approaches temperature of the emitted electrons.

For more info see J.P. Sheehan's PRL 2012, POP 2013
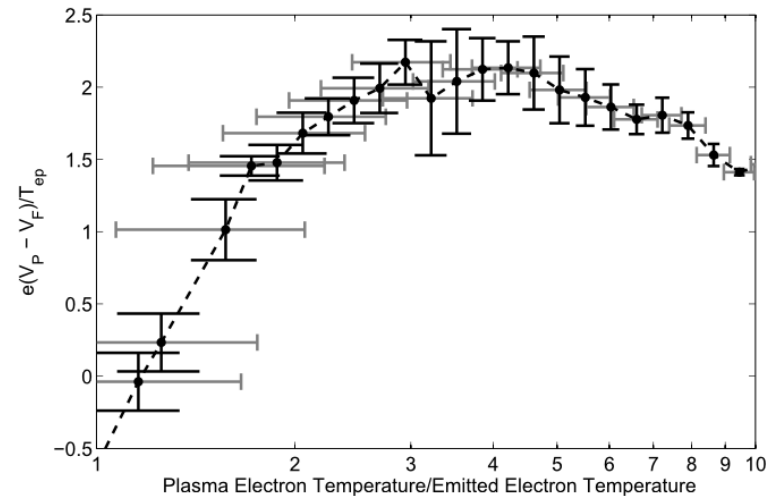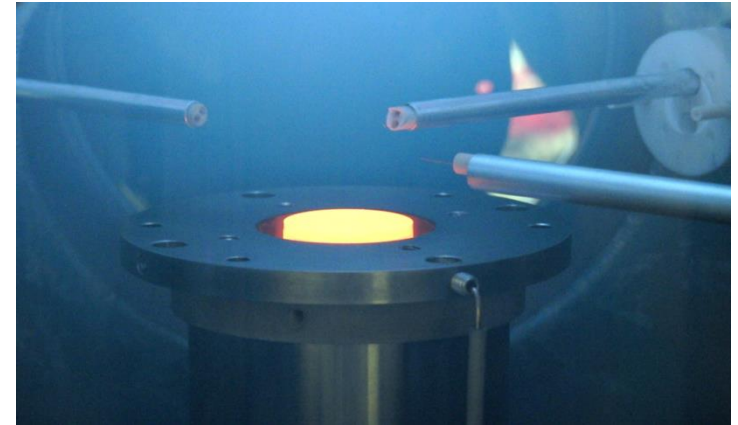
Plasma properties can be changed by applying engineered materials to the surface

Hall thruster
Inner wall electrode
Outer wall electrode
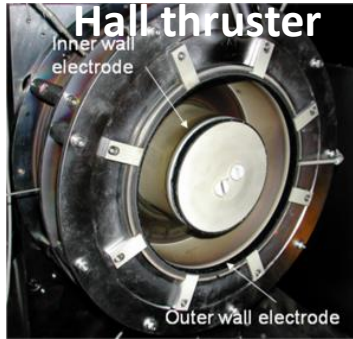
Application of carbon velvet to channel walls improves considerably thruster performance by reducing the electron cross-field current and by increasing nearly twice the maximum electric field in the channel compared with the conventional BN ceramic walls.

Velvet before plasma

Channel wall
Carbon velvet
Protrusive fibers $> \lambda_D$
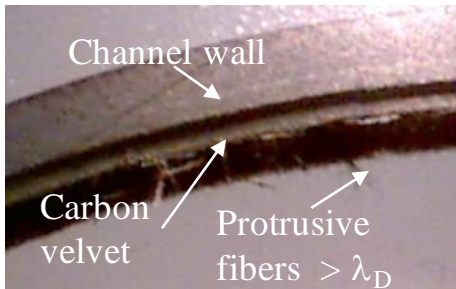
Plasma burned out all protrusive fibers

Carbon velvet

Plasma flow

Velvet Fibers
l_p
g
L
Wall
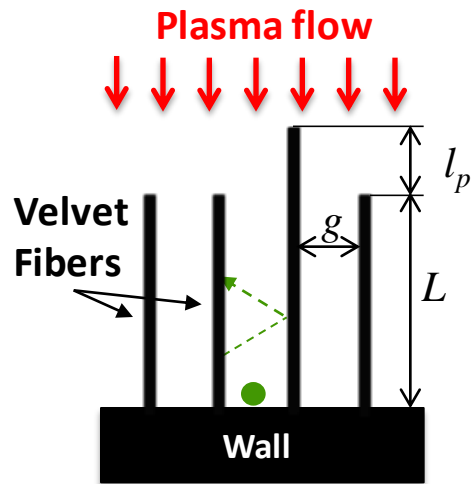
To avoid field emission $g, \; l_p <$ **Debye length**

High SEE boron nitride
Very low SEE velvet
Discharge current, A
Discharge voltage, V
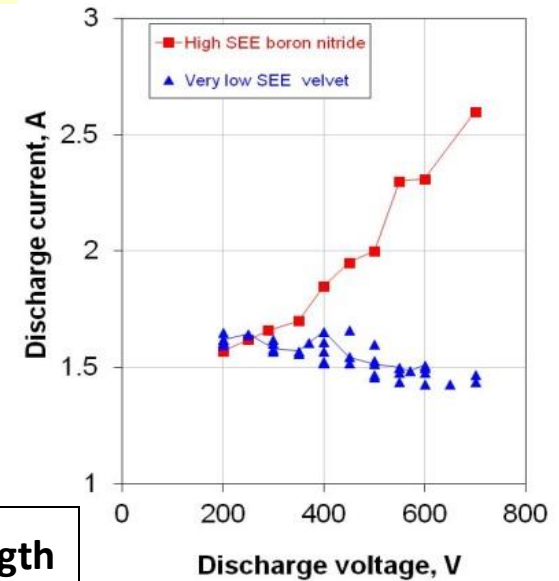
- **Velvet suppresses SEE and reduces current at high voltages (good)**
- **Sharp tips can enhance field emission leading to arcing (bad)**
- **Need to engineer velvet morphology so that inter fiber gaps and protrusions are located well inside the sheath to avoid damage by arcing**

    Need to take into account spatial and temporal variations of sheath width due to plasma non-uniformity or instabilities

19

Emission from complex surfaces
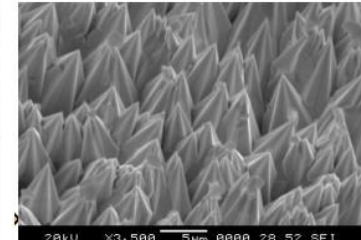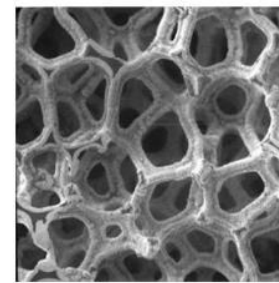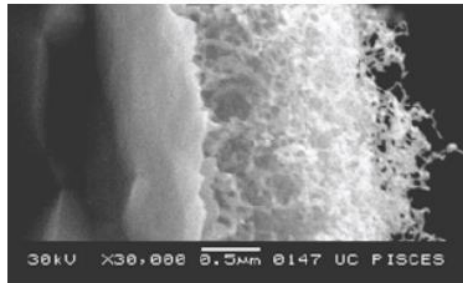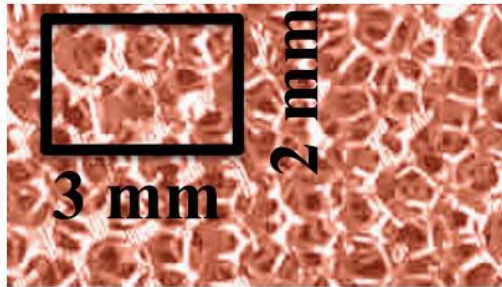
- Designed Matlab code to simulate complex shapes
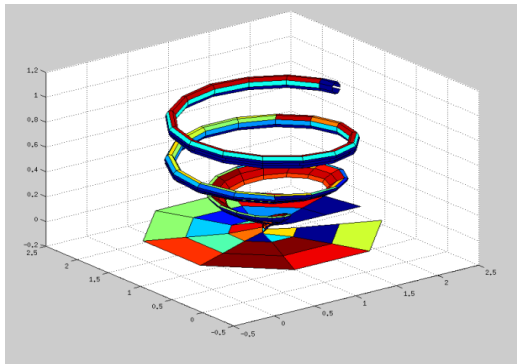
$\gamma=0.58\gamma_{flat}$
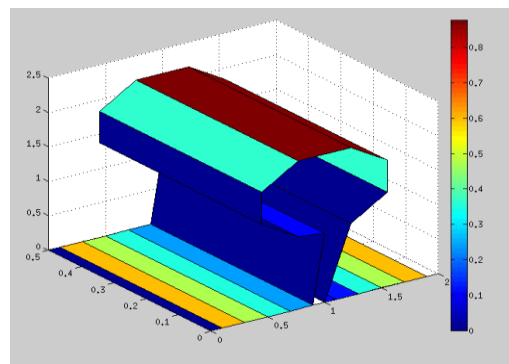
$\gamma=0.59\gamma_{flat}$
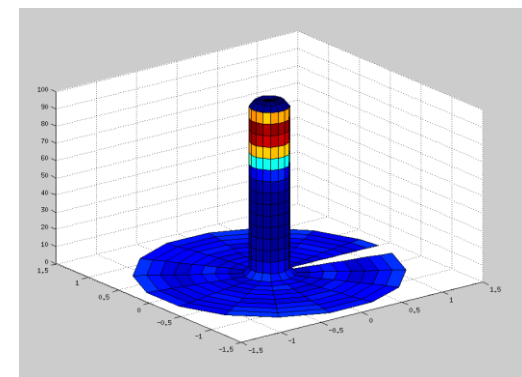
$\gamma=0.2\gamma_{flat}$

Calculation of Effective Secondary Electron Emission Yield from Velvet-like structures
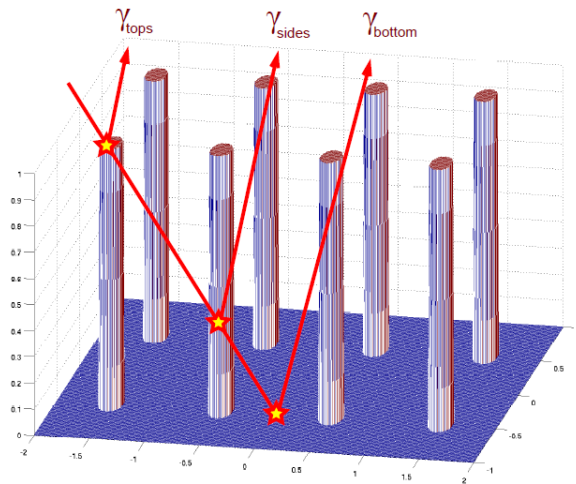
Fig.1 Contributions to the SEY emitted by the tops, sides and the bottom surface.

Exact analytic results vs approximate numerical results for SEY
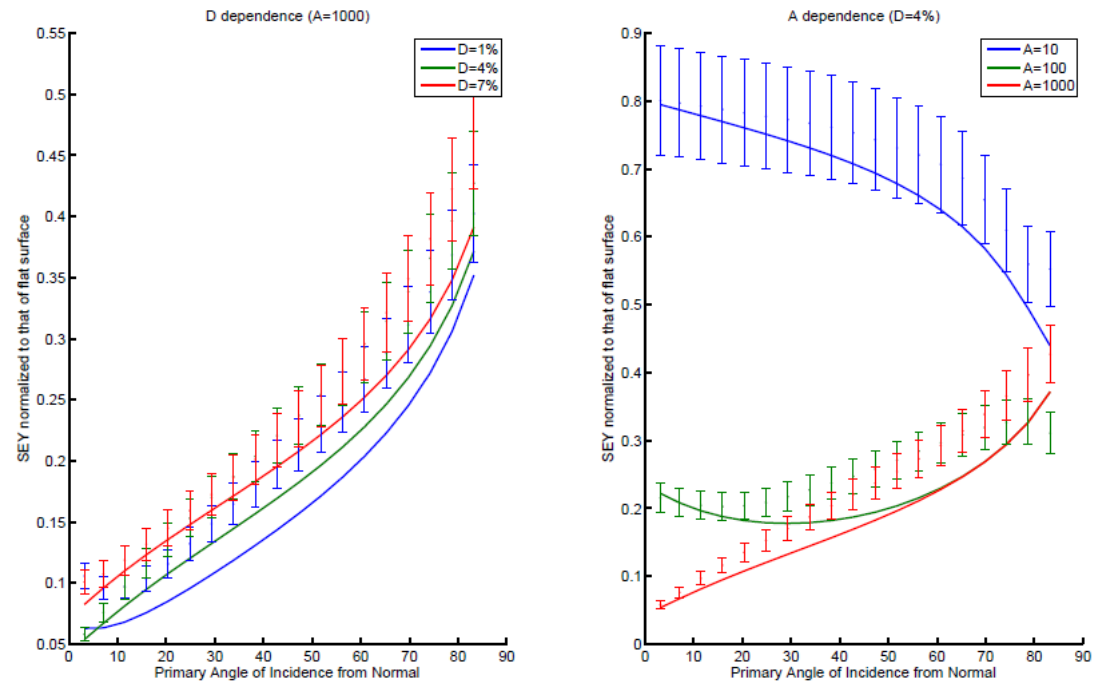
Fig.2. SEY vs angle of incidence for different values of aspect ration, A, and packing density, D.

Effects of Boundaries -- Revisiting Pierce Instability
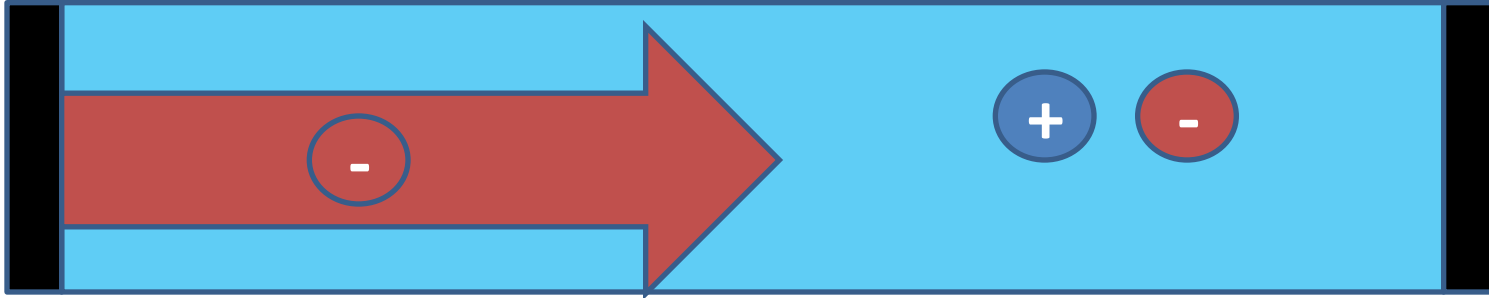
Electron beam is injected into electron and ion background of equal density.

Electrodes with fixed potential set potential at boundaries.

Instability is very different from textbook calculation for periodic b.c.

$$\omega_{e,0} \left(n_{b,0} / n_{e,0} \right)^{1/3}$$

$$\frac{\partial n_{e,b}}{\partial t} + \frac{\partial v_{e,b} n_{e,b}}{\partial x} = 0 \qquad \delta n_b(0) = \delta v_b(0) =$$

$$\frac{\partial v_{e,b}}{\partial t} + v_{e,b}\frac{\partial v_{e,b}}{\partial x} = -\frac{e}{m}E \qquad \delta\phi(0) = \delta\phi(L) = 0$$

$$\delta\phi(t,x) = \left(Ax + Be^{ik_+ x} + Ce^{ik_- x} + D\right)e^{-i\omega t},$$

the following additional relation between ω and k:

$$k_-^2\left(e^{ik_+ L} - 1\right) - \frac{ik_-^2 k_+ \omega L}{\omega - k_+ v_{b,0}} =$$

$$k_+^2\left(e^{ik_- L} - 1\right) - \frac{ik_+^2 k_- \omega L}{\omega - k_- v_{b,0}}.$$

(10)

$$k_\pm = (1 \mp \chi)\frac{\omega_{e,0}}{v_{b,0}}$$

$$-i\frac{2(1-\chi)}{(1+\chi)\chi}L_n + e^{i(1-\chi)L_n} - 1-$$

$$\frac{(1-\chi)^2}{(1+\chi)^2}\left[e^{i(1+\chi)L_n} - 1\right] = 0$$

Frequency (a), temporal growth rate (b), wavenumber (c), spatial growth rate (d), and the number of wave periods per system length (e) versus the length of the system.
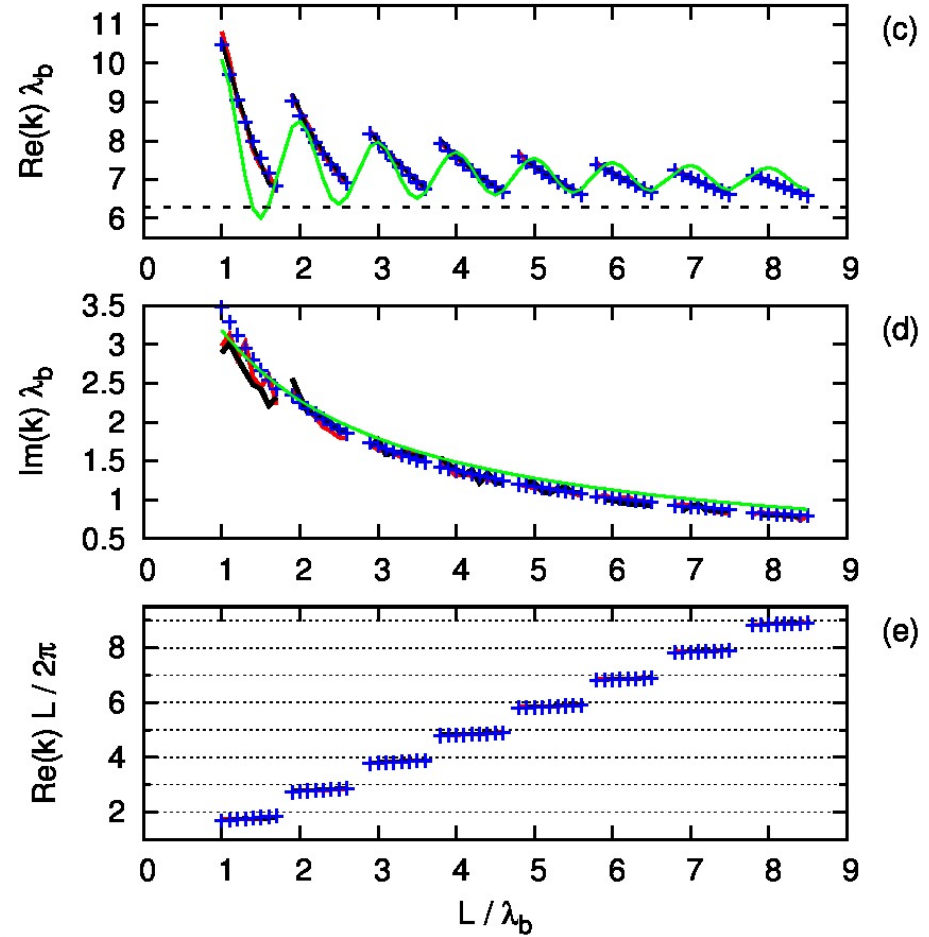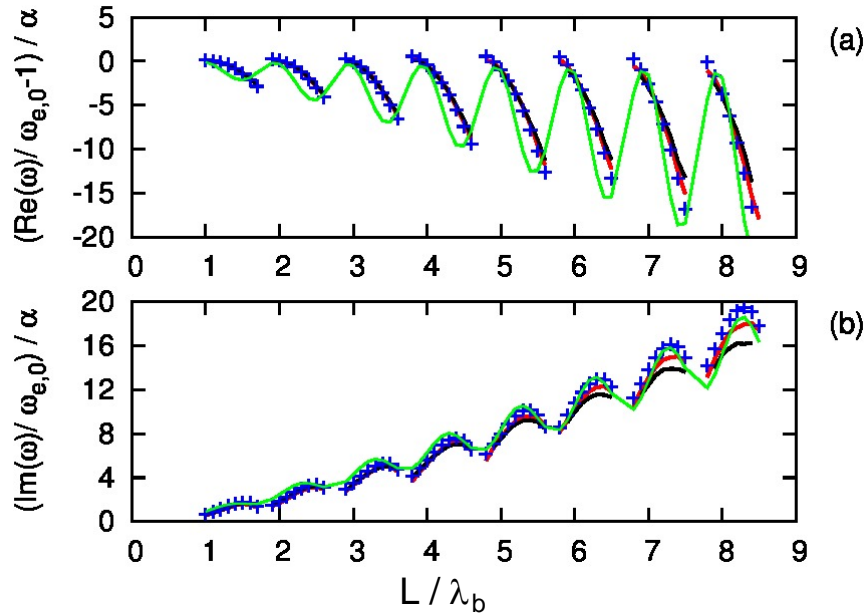
The blue crosses mark values obtained by analytical solution.

$$Im(\omega) \approx \frac{1}{13} L_n \ln(L_n) \left[1 - 0.18 \cos \left(L_n + \frac{\pi}{2} \right) \right] \alpha \omega_{pe},$$

where $L_n = L \omega_{pe}/v_b$, wavenumber $Re(k) \approx$

$\frac{\omega_{pe}}{v_b} \left[1 + \frac{1 + 2.5 \cos(L_n)}{1.1 L_n} \right]$. For comparison, the

classical values: growth rate $Im(\omega) = 0.7 \alpha^{1/3} \omega_{pe}$.

Solid red and black curves represent values obtained in fluid simulations with $\alpha = 0.00015$ (red) and 0.0006 (black). Solid green curves are values provided by fitting formulas. In (c), the black dashed line marks the resonant wavenumber.

Conclusions

- **SEE is important to take into account for many applications with Te>20eV for dielectrics and >100eV for metals.**

- **SEE strongly affect sheath. Instability due to EVDF-sheath coupling, inverse sheath**

- **Complex structures can reduce SEY. Theory was developed for optimal parameters of velvet.**

- **SEE can create beams of electrons penetrating the plasma and causing two-stream instability. We have studied the development of the two-stream instability in a finite size plasma bounded by electrodes both analytically and making use of fluid and particle-in-cell simulations. Its behavior is very different from infinite plasma.**

Developing Computational Capabilities for Thruster Simulations

J. Carlsson, A. Powis, I.D. Kaganovich, A.V. Khrabrov, Y. Raitses

Princeton Plasma Physics Laboratory, NJ

PPPL

PRINCETON
PLASMA PHYSICS
LABORATORY

Particle-in-cell codes can resolve complex micro physics and complex geometry

An electrostatic parallel, implicit, 1D PIC code EDIPIC. Implemented electron-atom scattering, ionization, and excitation as well as electron-ion and electron-electron collisions, electron induced emission.

3D LSP code also includes electromagnetic and electrostatic modules.
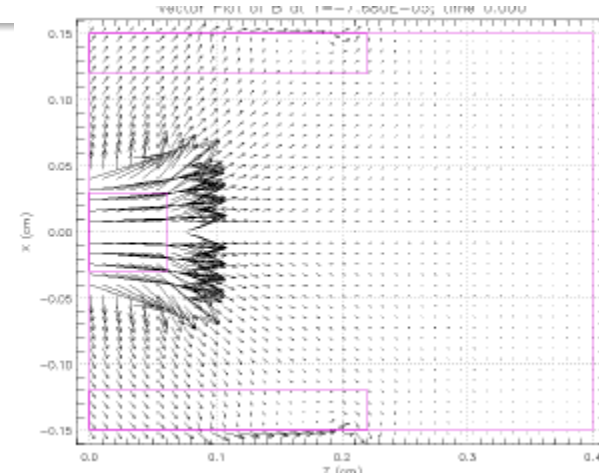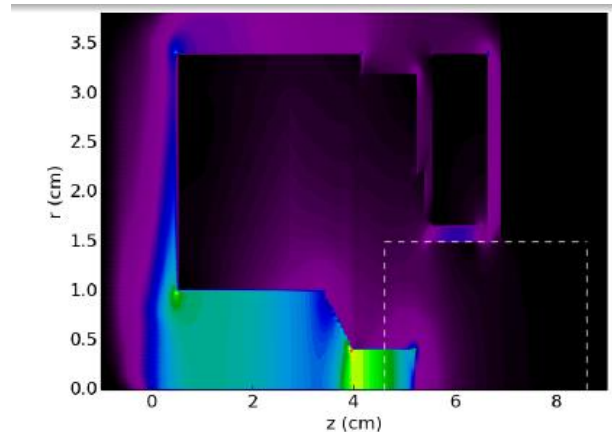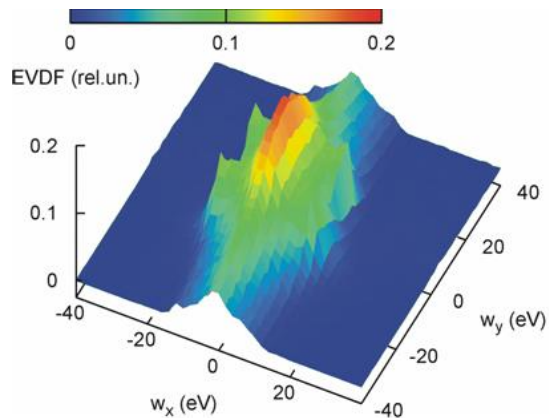
D. Sydorenko, *et al*, Phys Rev Lett., 103 145004 (2009).

Improvements in lsp code

- **LSP code 3D - Electrostatic and Electromagnetic Particle-In-Cell code includes:**
  - **Implicit, Explicit Electrostatic and Electromagnetic solvers**
  - **Full collision algorithm for isotropic elastic and inelastic collisions.**
- **Improvements:**
  - **New Electrostatic PETSc Solvers**
  - **Anisotropic elastic and inelastic collisions**
  - **External circuit**

Benchmarking of codes

E. A. Den Hartog, D. A. Doughty, and J. E. Lawler, "Laser optogalvanic and fluorescence studies of the cathode region of a glow discharge", Phys. Rev. A 38, 2471 (1988).
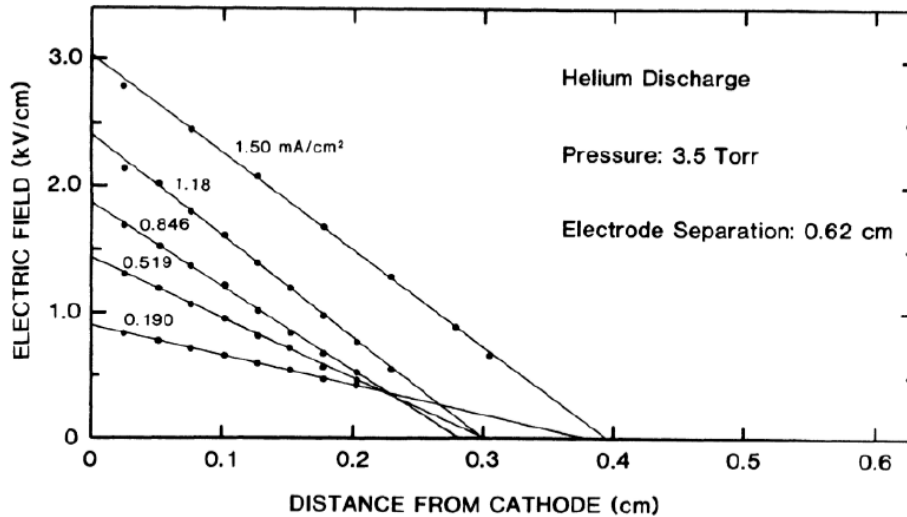
Accurate and complete measurements of the plasma quantities: E(x), γ, J, U.

For more info see J. Carlsson, PSST 2016
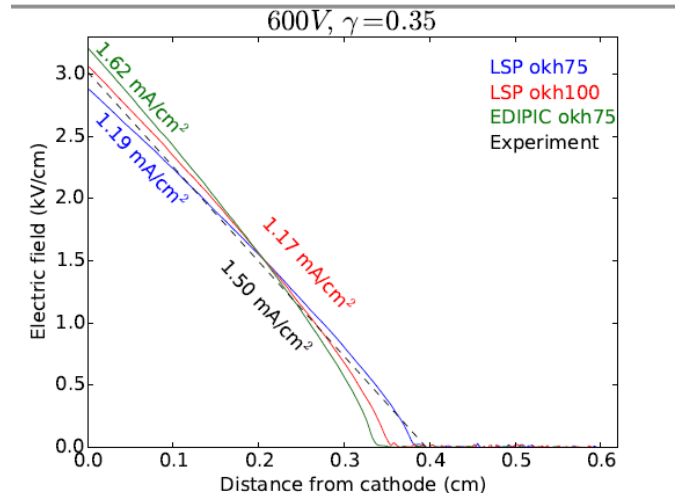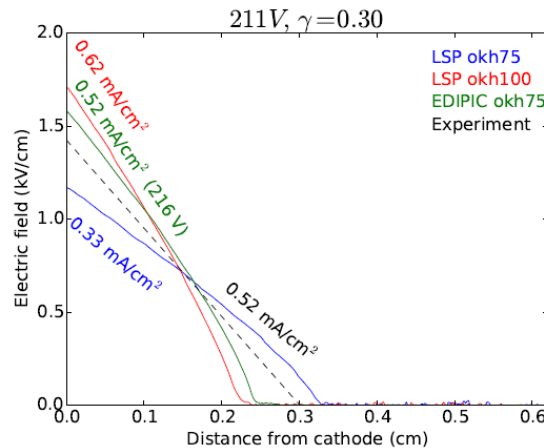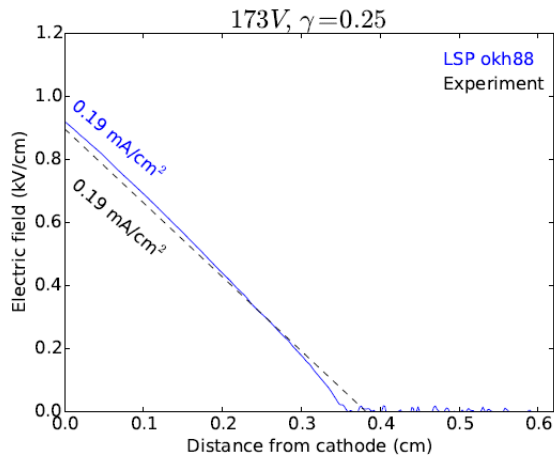
Part 2: Control of particles distribution functions using external magnetic field

- **The application of the magnetic field can greatly modify the EEDF in a low pressure plasma:**

  - **Ionization can be localized.**

  - **Separation of plasma regions with hot and cold electrons (so-called magnetic filter).**

  - **Anisotropy in electron motion along and across B.**

  - **Control of the electric field in plasma.**

- **Applications of the magnetic filter: positive and negative ion sources, neutral beam injectors, and plasma thrusters, plasma processing**
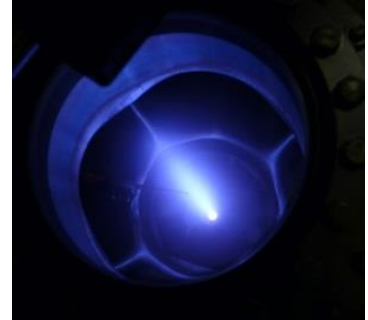
Results of spoke-simulations in 2D

Anomalous transport in 2D is very robust and is much larger than collisional transports. A solid-body rotating structure is observed as shown in movie:

Penning2D-ni
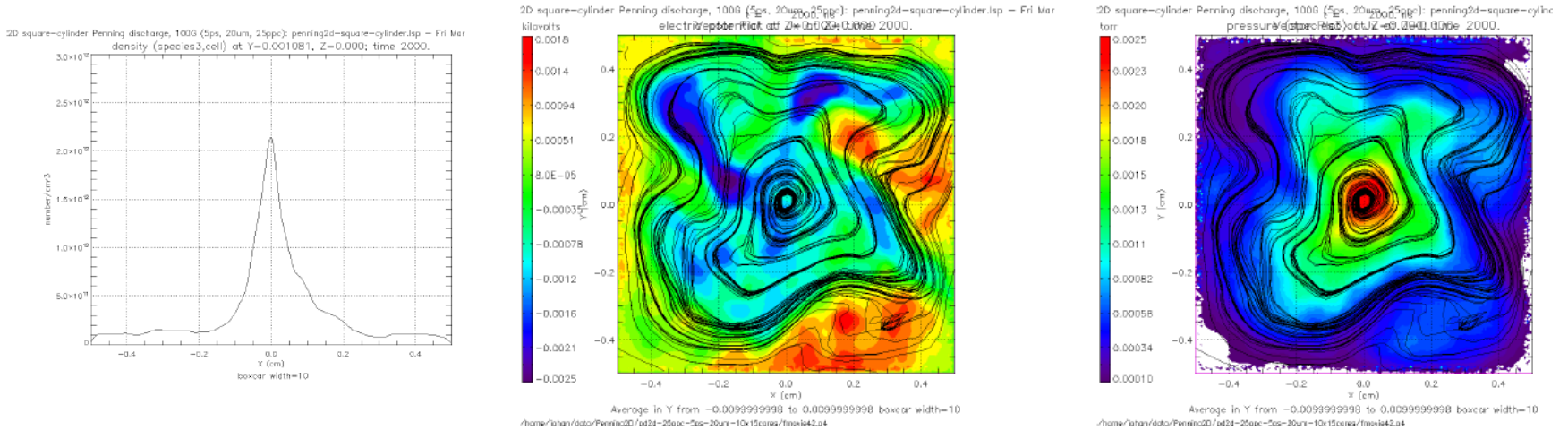
Density is peaked in the center, similarly to 1D but reaches to the sheath region as opposite to 1D. Current streamlines on top of potential contours (middle) and electron-pressure contours (right) at 2 μs.

Results of spoke-simulations in 2D
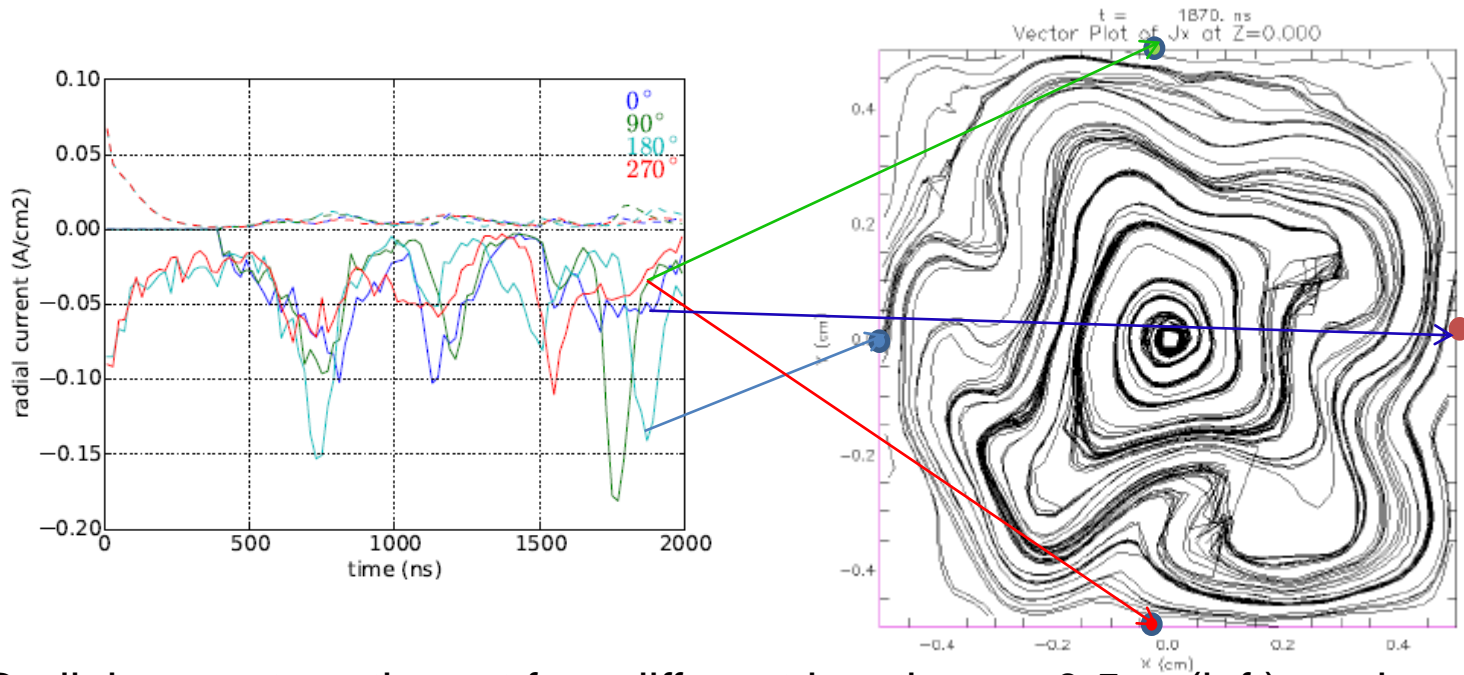
Radial current vs. time at four different locations r=0.5cm(left) and current streamlines (right) at 1870ns.

The radial current exhibits bursts at the spoke frequency, see Fig.. When a current burst occurs, one would expect current stream lines from the interior plasma to connect with the wall as evident in Fig. , for 180°. Other streamlines are parallel to the wall at the top (90) and the bottom (270), resulting in minimal radial current at those locations.
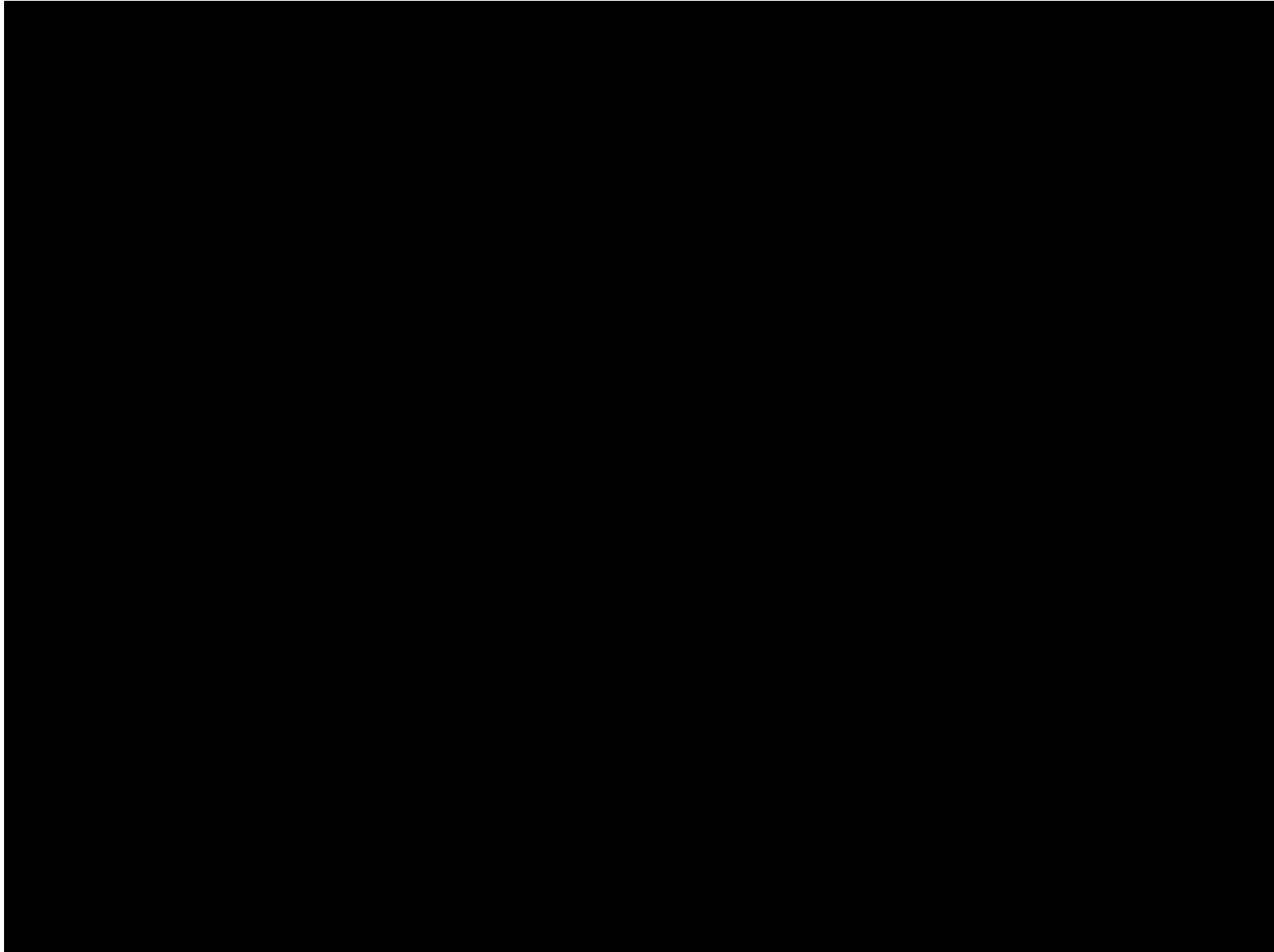
Effective transport
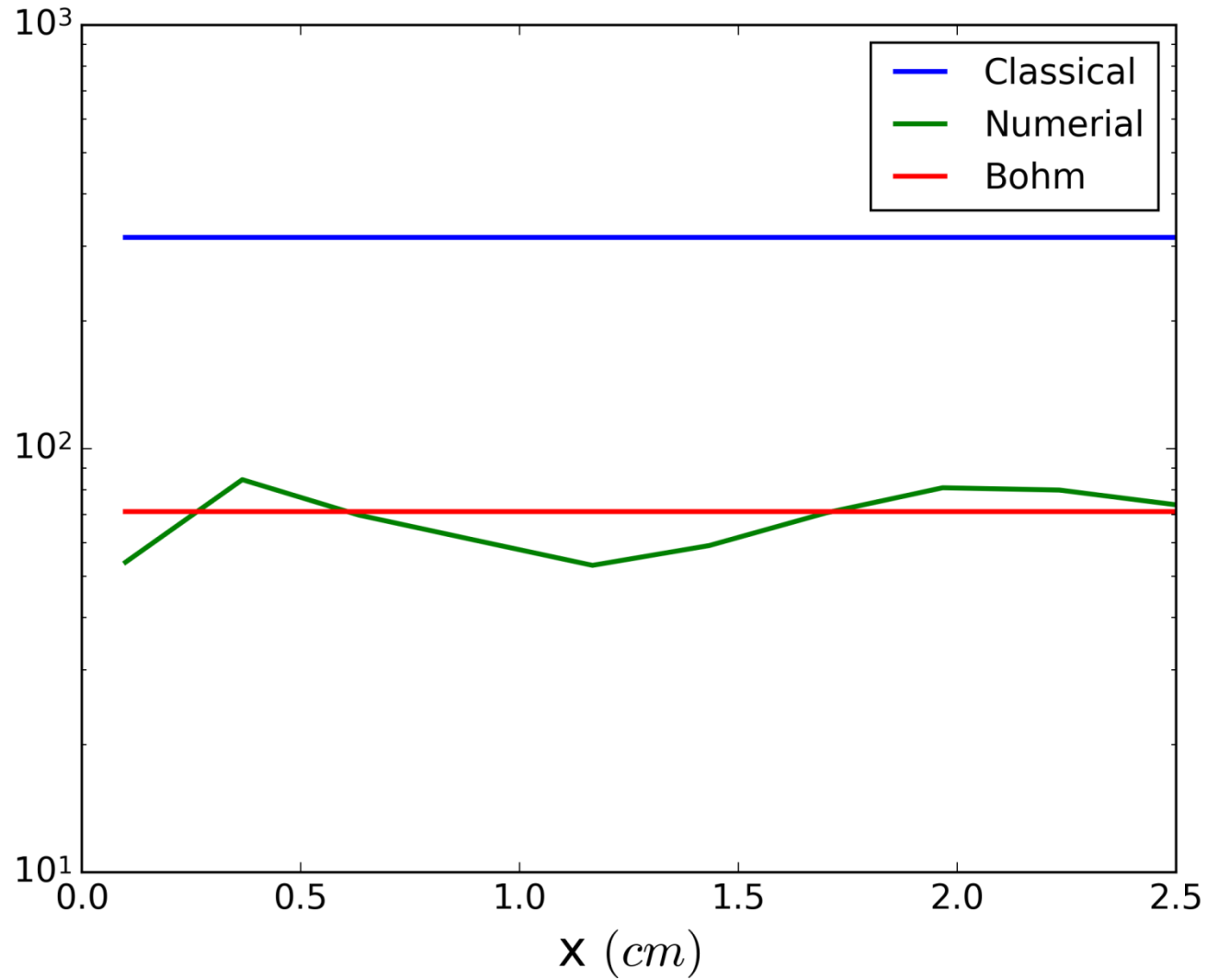
Summary of Part 2

- We studied a number of low pressure E×B discharges with weakly collisional quasi-neutral plasma, including plasma lens, Penning discharge and Hall thrusters of different configurations.

- All these plasma discharges are characterized by anomalously high (not collisional) electron cross-field transport.

- Anomalous transport is predicted to be due to small and large scale instabilities.

- An example of large scale instability is the E×B rotating spoke.

  - Recent PIC simulations predict small scale instabilities inside the spoke.

- Spoke can be controlled and suppressed with a feedback circuitry.

Effect of Surface Architecture on Secondary Electron Emission Properties of Materials

Yevgeny Raitses and Igor Kaganovich

- Strong SEE effects on plasma-wall interaction occur when SEE approaches 1 (top figure).

- For ceramic materials, SEE yield is higher and approaches 1 at lower energies than for metals due to a weaker scattering of SEE electrons on phonons (for insulators), $\lambda \sim 20$ nm, than on electrons (for metals,), $\lambda \sim 1$ nm.

- Surface-architectured materials can reduce the effective SEE yield by trapping SEE electrons between surface structural features.

- The SEE reduction is most significant for high aspect ratio (1:10^3) velvets than for low aspect ratio (1:10) dendritic coatings (top figure).

- Measurements demonstrate the existence of the optimum aspect ratio and the density of the architectural features (bottom left figure).

- New result: surface architecture affects the energy distribution function of emitted electrons reducing the fraction of backscattered electrons –important for collisionless plasmas used in EP (bottom right figure).
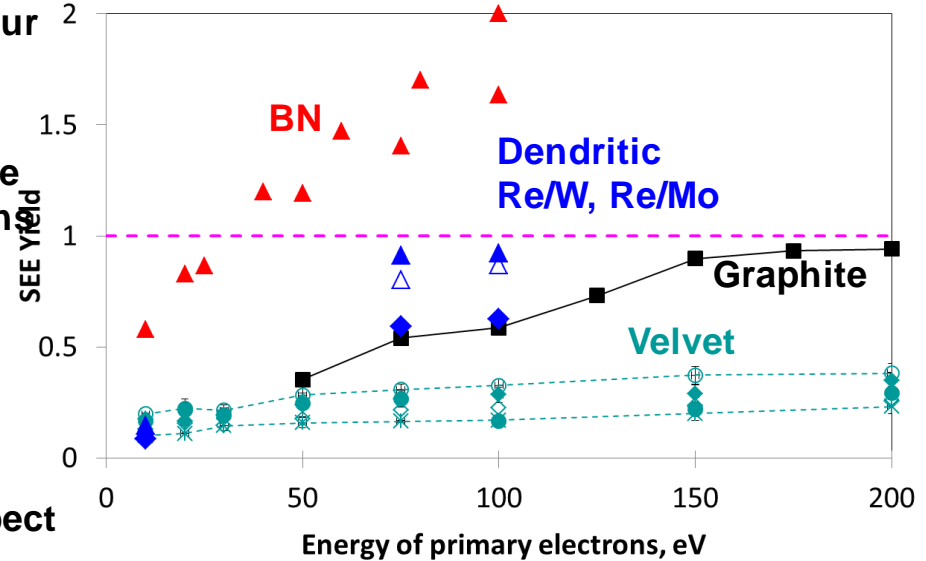
Carbon Velvet: Effect of fiber length and packing density on SEE for beam electrons of **50 eV** and
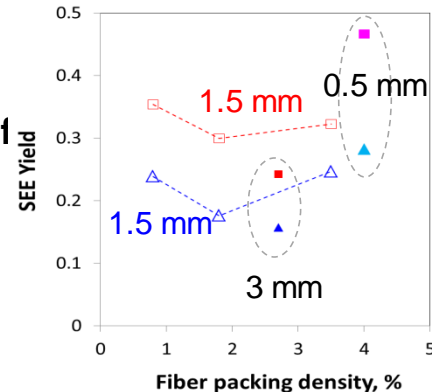
Fractions of true and back scattering SEE electrons measured for velvets (green) and graphite (black)
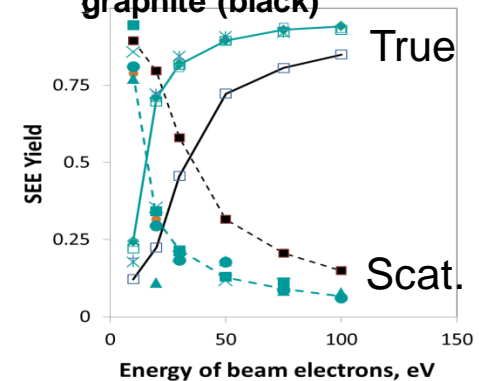
Calculation of Effective Secondary Electron Emission Yield from Velvet-like structures

Fig.1 Contributions to the SEY emitted by the tops, sides and the bottom surface.

Fig.2 Analytic Secondary Electron Yield normalized to that of a at surface, including the approximate optimal D value in magenta.

$$D_{optimal} \approx \frac{C_0}{A} + C_1 \frac{ln(A)}{A} (\tan \theta_1)^{C_2}$$

e $C0 = -0.1, C1 = 0.97, C2 = -0.6$ give the best agreement with 10% average error.

Evolution of the bulk electron density perturbation in time and space in fluid; Solid black lines in represent propagation with the unperturbed beam velocity. Dashed black lines in represent phase velocity of the wave calculated analytically.
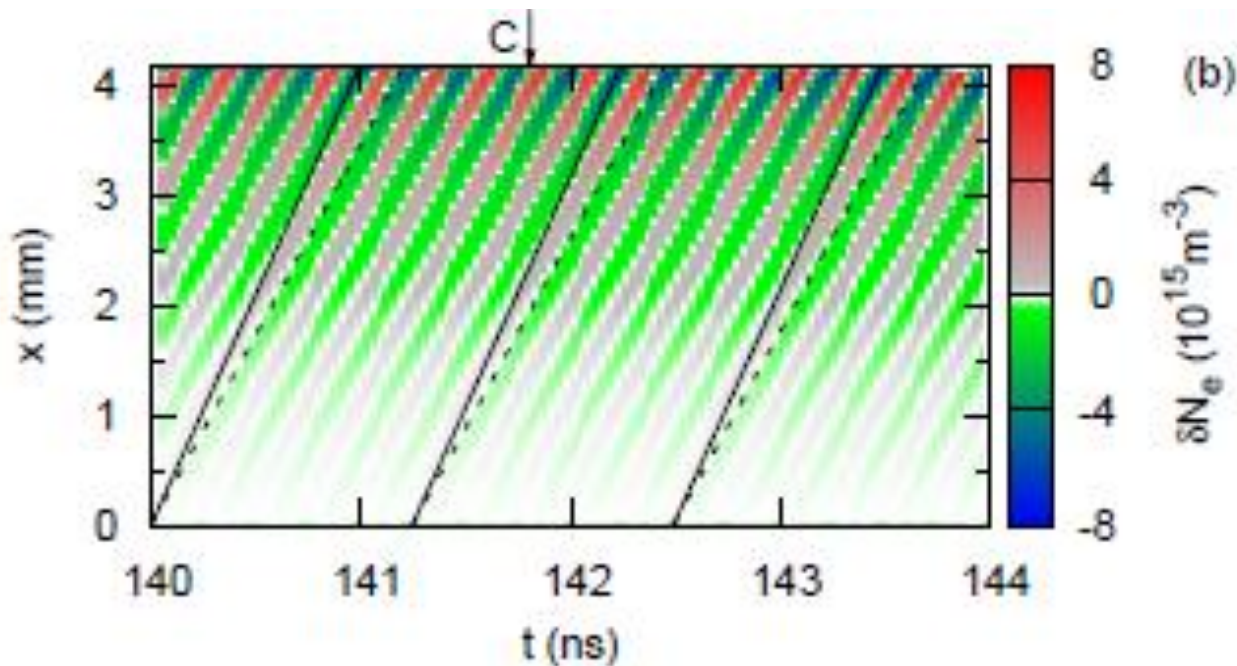
EFFECT OF COLLISIONS ON THE TWO-STREAM INSTABILITY IN A FINITE LENGTH PLASMA

Collisions of plasma bulk electrons further reduces this growth rate. The rate becomes zero if the collision frequency is equal to the doubled growth rate without collisions.

$$Im(\omega) = Im(\omega_{ncl}) - \nu_e/2 \ .$$

$$Im(\omega_{ncl}) \approx \frac{1}{13} L_n \ln(L_n) \left[1 - 0.18\cos\left(L_n + \frac{\pi}{2}\right) \right]$$

FIG. Phase plane "emission current density vs neutral gas pressure". The dashed black straight line is the analytical threshold current plotted using these threshold pressure values.
n = 2·10^{11} cm^{-3}, L = 1.85cm,
Beam energy = 800 eV.

$$J_{b,thr} = \frac{6.5\kappa(T_e)\sqrt{2e\varepsilon_0 n_{e,0}W_{b,0}}}{L_n \ln(L_n)\left[1 - 0.18\cos\left(L_n + \pi/2\right)\right]} p_n$$

Pressure should be less than P=15mTorr for the beam current $J_{b.thr} = 5.4mA/cm^2$ **to observe the instability.**

IMPROVEMENTS IN EDIPIC CODE

- **EDIPIC code - Electrostatic Direct Implicit Particle-In-Cell code includes:**
  - **Implicit Poisson solver**
  - **Null collision algorithm for anisotropic elastic and inelastic collisions, electron-electron collisions, EVDF diagnostics, wave spectrum diagnostics, wall electron emissions**
- **Improvements:**
  - **Magnetic field at an arbitrary angle to walls**
  - **Full collision algorithm**
  - **External circuit**

PRELIMINARY RESULTS OF SPOKE-DRIVING EXPERIMENTS

- **Azimuthal modes can be driven in both ExB and –ExB direction.**

- **Frequency of azimuthal modes exactly follow driving frequency in the range 10 KHz-50 KHz.**

- **Coherence of the azimuthal modes depends on driving frequency.**
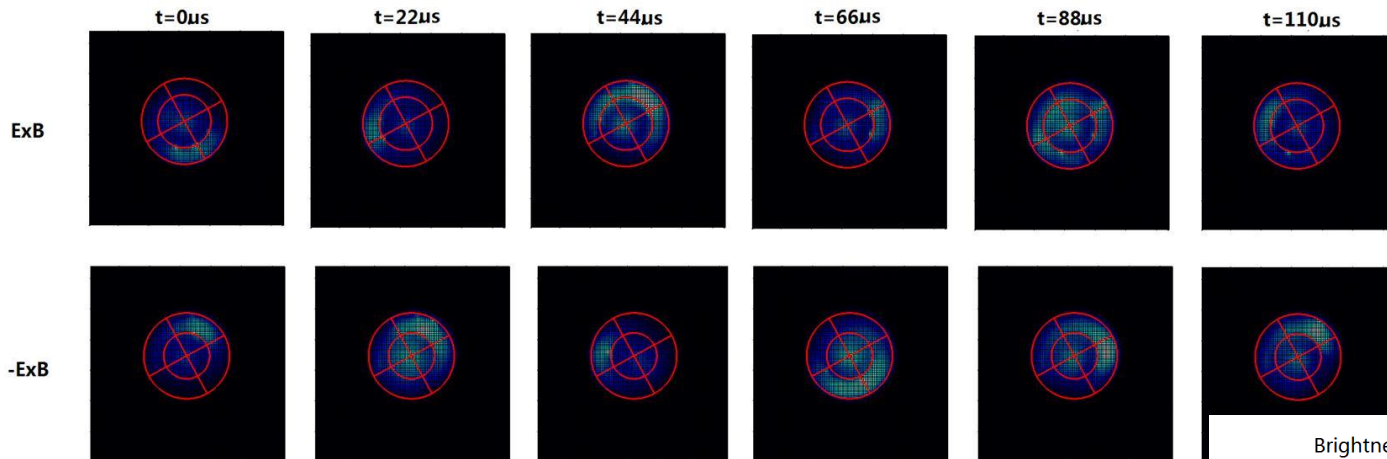
- **Sequence of high speed camera images showing a spoke of increased light emission driven artificially in a segmented anode Hall thruster.**
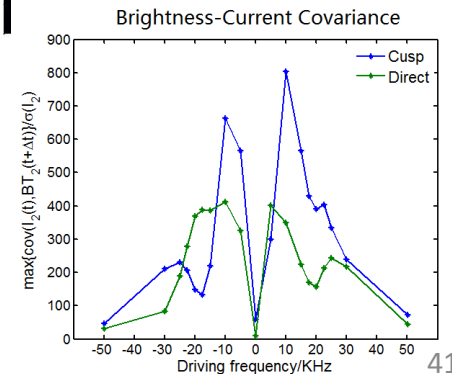
Penning-type E×B configuration of beam-plasma system
Y. Raitses PPPL

Device creates hot electrons in the center and cold on a periphery.

E-field is determined by B-field and magnetic field surfaces are equipotentials.

E×B configuration designed to create the electron beam propagating in plasma.

Operating parameters and configuration:

  Xenon and Argon. Pressure: 0.1-10 mtorr

  Magnetic field: 50-200 Gauss

  $$R_{Le} << L < R_{Li}$$

  Cathode current: 2 A Voltage: 50-100 V

  Ceramic side walls

Xenon operation